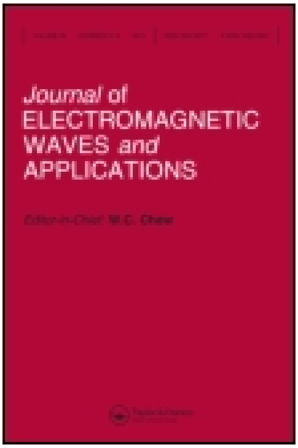

Journal of Electromagnetic Waves and Applications
Publication details, including instructions for authors and subscription information:
http://www.tandfonline.com/loi/tewa20

Substrate Integrated Waveguides with Moats

R.-B. Hwang [a] & C. Y. Chin [b]

[a] Department of Electrical Engineering, National Chiao-Tung University, 1001, Da-Hsueh Road, 300 Hsinchu, Taiwan, Republic of China

[b] Department of Electrical Engineering, National Chiao-Tung University, 1001, Da-Hsueh Road, 300 Hsinchu, Taiwan, Republic of China

Published online: 03 Apr 2012.

J. of Electromagn. Waves and Appl., Vol. 23, 1101–1112, 2009

SUBSTRATE INTEGRATED WAVEGUIDES WITH MOATS

R.-B. Hwang and C. Y. Chin

Department of Electrical Engineering
National Chiao-Tung University
1001, Da-Hsueh Road, 300 Hsinchu, Taiwan, Republic of China

Abstract—A substrate integrated waveguide (SIW) equipped with moats is investigated in this paper. Different from the commonly used SIW having dense via holes, this new SIW employed sparse via holes incorporating moats outside the via-hole arrays. Through numerous experimental studies, we found that it can maintain high transmission characteristics by introducing additional moats outside the via-hole arrays. Moreover, it is interesting to notice that such a new structure can lower its cutoff frequency and thus increase its operation bandwidth. Additionally, the calculation for the dispersion relation of such a new waveguide was carried out to understand its wave-guiding characteristics.

1. INTRODUCTION

The substrate integrated waveguide (SIW) or post-wall waveguide technique was developed to fabricate an equivalent rectangular waveguide on a low-loss microwave substrate [1–9]. Such a class of waveguide was proved to be able to preserve the advantages of commonly used metallic rectangular waveguide; for example, the high-Q factor. Since the SIW is fabricated using standard printed-circuit board (PCB) technique, it is easy to be integrated with a planar transmission line circuit, such as the microstrip line, coplanar waveguide and slot line. Moreover, unlike the traditional metallic waveguide, this waveguide can be fed by a tapered transition microstrip line instead of a complicated three-dimensional coaxial probe.

Analytical approach to determine the complex propagation constant of SIW with lossy dielectric was proposed using the

Corresponding author: R.-B. Hwang (raybeam@mail.nctu.edu.tw).

generalized multipole technique (GMT) [10]. Meanwhile, modal analysis was adopted to investigate the loss mechanisms including dielectric, conductor and radiation loss [11]. Recently, SIW has attracted much interest in the design of microwave and millimeter-wave integrated circuits. Numerous SIW components such as filters, multiplxers and power dividers have been studied. A novel SIW bandpass filter has raised the Quality factor to around 150 [12]. Bandpass filters cooperating cavity or complimentary split ring resonator (CSRR) on SIW were designed [13–15]. Specifically, the realization of broadband bandpass filter was achieved by combining both highpass and bandstop characteristics on half mode substrate integrated waveguide (HMSIW) [16]. A new generalized Chebyshev SIW diplexer was presented for high performance which possessed of the advantages of both SIW and the generalized Chebyshev filters [17]. On the other hand, feeding network utilizing compact SIW binary divider has also been developed to feed antenna array printed on thick substrates [18].

Additionally, the theoretical investigation concerning the guided-wave and leaky-wave characteristics of SIW was treated using various numerical methods, such as finite-difference frequency domain method [7] and numerical multimode calibration procedure incorporating the finite element method [8, 11]. An accurate empirical formula of the equivalent rectangular waveguide width was developed to provide design criteria; for example, the ratio of pitch distance to via-hole diameter. Since the waveguide wall is made by the via-hole array, energy shall leak from the space between two via holes into the surrounding substrate if the distance between two adjacent via holes is too large. To avoid the energy leakage, two or more via-hole arrays were employed to enhance reflectivity of the waveguide side walls. As was indicated in [7], when the ratio of p to r is smaller than 4.0 and that of w to r is larger than 8.0, the SIW can be equivalent to a commonly used rectangular waveguide; where w, r and p are the width, radius of via hole and pitch distance (distance between two via holes), respectively, shown in Fig. 1. In this research, a new structure having moats outside the sparse via-hole arrays was developed. As depicted in Fig. 1, we increase pitch distance and add two moats (slits) outside the via-hole arrays. From the measured and calculated results, we found this new structure can considerably reduce leakage loss and retain the high transmission property compared with the waveguide with dense via holes. Moreover, we found that such a waveguide has a lower cutoff frequency than that of the commonly used one. Therefore, this new waveguide provides a wider bandwidth than the traditional one.

Besides, such a new structure can reduce power leakage from the

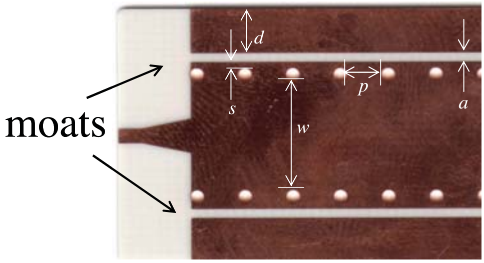

Figure 1. Structure configuration of the post-wall waveguide with moats where $p = 3\,\mathrm{mm}$, $a = 0.75\,\mathrm{mm}$, $r = 0.5\,\mathrm{mm}$, and $s = 0.54\,\mathrm{mm}$, $d = 3.74\,\mathrm{mm}$, and $w = 9.15\,\mathrm{mm}$, respectively. The dielectric substrate used here is RO4003 with relative dielectric constant 3.55.

guided channel into the surrounding parallel-plate regions and further suppress cross-talk (or electromagnetic coupling) between neighboring waveguides. It provides a possibility for integrating SIWs, passive and active components in a substrate while mitigating the electromagnetic interference. In addition to the numerical simulation and experimental measurement for the scattering parameters of this new waveguide, we have calculated the dispersion relation of the waveguide including the phase- and attenuation-constant for understanding the physical picture of wave process in this guided-wave structure.

2. STRUCTURE CONFIGURATION

The structure and picture of the new SIW under consideration are shown in Fig. 1. It consists of two tapered microstrip lines transitioning to SIW for reducing reflection of incident microstrip line mode at two ends of waveguide. The waveguide side wall was made by realizing via-hole arrays on the substrate using an electroplating technique. Different from the commonly used SIW, the new structure contains two moats with the width denoted by a outside the via-hole arrays. The microwave low loss substrate used here is RO4003 with relative dielectric constant 3.55.

3. EXPERIMENTAL STUDIES AND NUMERICAL SIMULATIONS

Figure 2 demonstrates reflection- and transmission-coefficient versus frequency for the traditional and new structure developed in this research with the same length of waveguide (37 mm). The first case

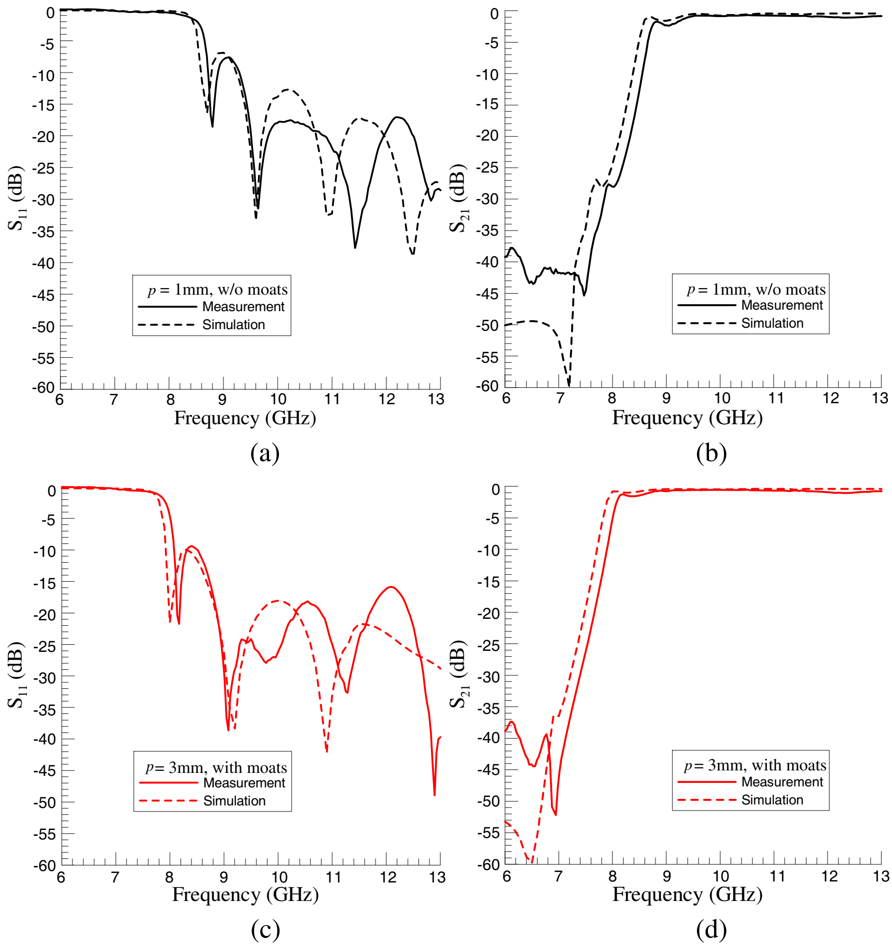

Figure 2. Distribution of reflection and transmission coefficients (in dB) versus frequency for the SIW with and without moats, respectively; (a) measurement, and (b) numerical simulation.

is the commonly used SIW with dense via-hole arrays with 1 mm pitch width shown in Figs. 2(a) and 2(b); the second one is the new SIW with pitch width 3 mm and moat width 0.75 mm shown in Figs. 2(c) and 2(d). We obtain the simulation results using time-domain simulation software: CST Microwave Studio. The results of the two cases are drawn in black- and red-color, respectively. Due to a considerable substrate loss for RO4003 after 13 GHz, measurement was taken up to 13 GHz. Comparing the numerical results with those of measured ones, we found that the numerical and measured results, in general, agree well for the two cases shown in this example. Notably, in the numerical simulation, the relative dielectric constant is assumed to be a constant (3.55) for the frequency range of operation. Since the dielectric constant is frequency dependence (dispersive), the calculated and measured results in S_{11} shows an obvious difference in groove.

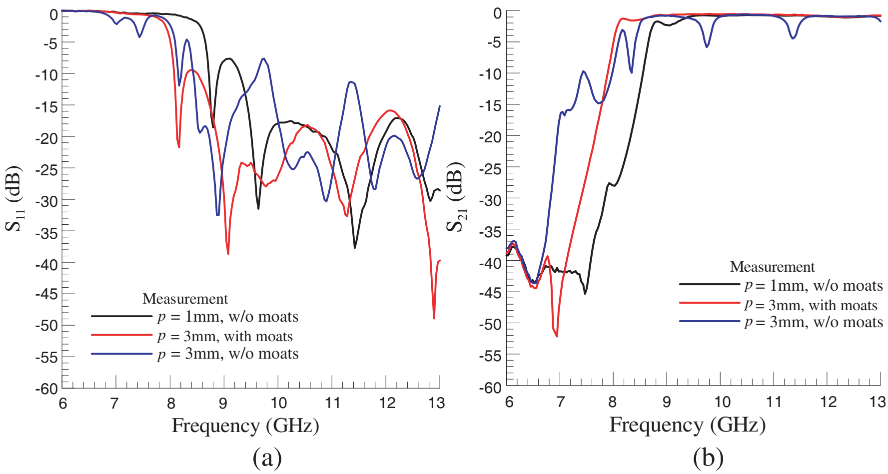

Figure 3. Measured reflection and transmission coefficients for three different SIW structures.

Figure 3 shows the measurement of SIWs fabricated in three different dimensions. Although two cases have been discussed previously, we add the third case here to make the comparison between them more distinguishable, which is the commonly used SIW with pitch width 3 mm. In this figure, the SIWs having the same pitch width 3 mm with and without moats are shown in red- and blue-color, accordingly. Even though the via-hole array becomes sparse, the moated SIW enhances the reflection- and transmission-loss significantly by simply etching two moats on the printed-circuit board.

We have explored the effect of s and d (their definitions were shown in Fig. 1) on the S_{11} and S_{21}, and the results are depicted in Fig. 4. As shown in Figs. 4(a) and 4(b), the cases with moat width 0.54 mm and 1.54 mm has insignificant changes on their scattering parameters. However, the last two cases show dramatic fluctuations. We may conjecture that for the case with large s the destructive interference between the reflected waves from the moat and via-hole array is significant. It may cause obvious fluctuation in the scattering parameters.

Additionally, the variation of scattering parameters against the changes in the distance d was shown in Figs. 4(c) and 4(d). Apparently, for a small distance s the effect of d on the scattering parameters is inconsiderable. Owing to almost the same position of the via-hole array and moat, the wave is totally reflected by this perfect reflection mirror. Thus, the good performance in the return- and insertion-loss was obtained.

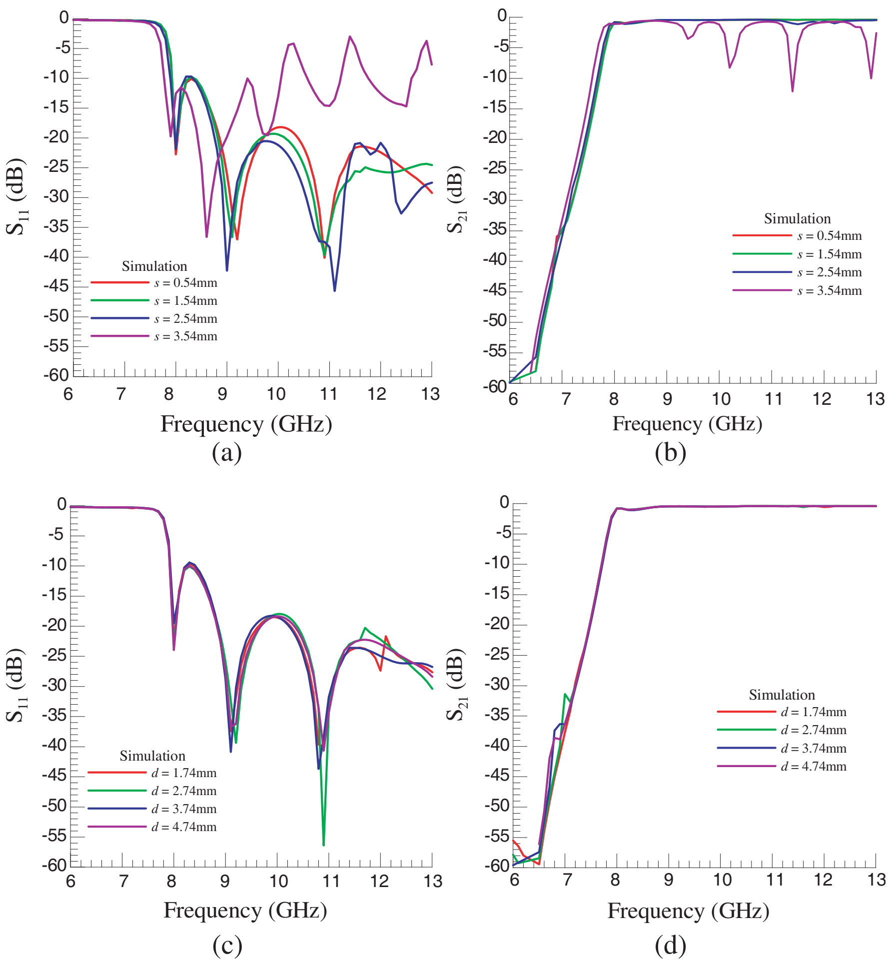

Figure 4. Distribution of reection and transmission coefficients (in dB) versus frequency for the SIW where s varies in (a), (b) and d varies in (c), (d).

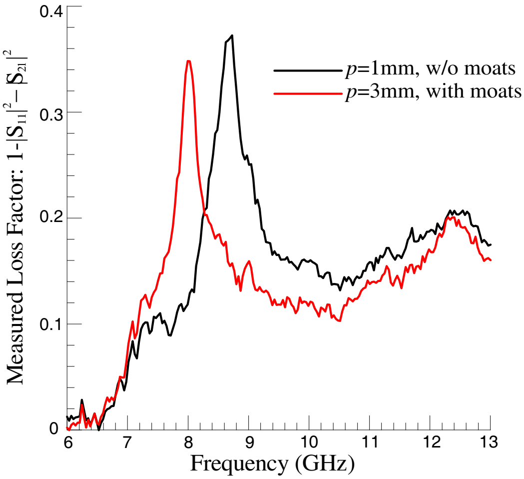

Figure 5. Measured loss factor of the SIW with and without moats, respectively.

For the new SIW with moats, the transmission response, generally, has better performance than that of the commonly used SIW. Specifically, such a new structure has a lower cutoff frequency compared with the traditional one, and thus has a wider bandwidth than that of the commonly used one.

In addition to the return- and insertion-loss, we also calculated the loss factor of the two waveguides described previously by evaluating $1.0-|S_{11}|^2-|S_{21}|^2$. As was shown in Fig. 5, the new SIW with moat, in general, has lower loss factor compared with the traditional SIW with dense via-hole arrays. The physical consequences can be explained in the following manner. Regarding the traditional SIW without moats, in addition to the surface current flowing through the via holes into ground plane, the surface current can also pass through the via-hole array and into the surrounding parallel-plate region, resulting in an excitation of parallel-plate waveguide modes. Therefore, the placement of moats outside the via-hole arrays can break the current path flowing into the parallel-plate regions and, meanwhile, suppress the excitation of parallel-plate waveguide modes.

The contour plot of electric field is depicted in Fig. 6, and each wave packet is half wavelength long in the corresponding guiding structure. It's easy to see that β/k_o is equal to $300/f\lambda_g$, where f is the frequency in GHz and λ_g is one guided-wave wavelength. As a result, we can utilize this formula to calculate β/k_o to an approximate extent. Since the pitch width and via radius of these two structures are given,

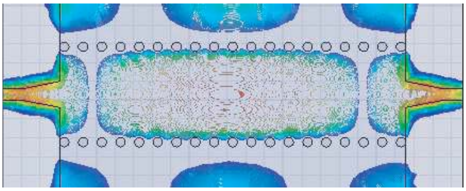

(a)

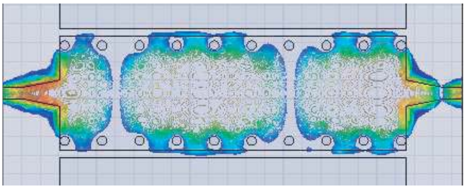

(b)

Figure 6. Contour map of electric field for (a) the traditional ($p = 1\,\text{mm}$, without moats) and (b) new ($p = 3\,\text{mm}$, with moats) SIWs while the operating frequency is 9 GHz.

in this case, pitch widths are 1 mm and 3 mm respectively with the same via radius 0.5 mm. By observation, the guided-wave wavelengths are 47 mm and 33 mm each. On the other hand, the corresponding β/k_o are 0.71 and 1.01 at 9 GHz which can be verified by Fig. 7.

The substrate integrated waveguide employs the via-hole array as its waveguide side wall. Therefore, the waveguide modes supported in this waveguide are rectangular waveguide modes with obvious cuto phenomenon as shown in the dispersion characteristics. Specifically, since the via-hole array and moat were utilized simultaneously, the combination of E-wall (via-hole arrays) and H-wall (moats) results in the waveguide mode has a cutoff frequency lower than that of the commonly used rectangular waveguide.

As far as a waveguide is concerned, the guiding characteristic including phase and attenuation constants is the most important factor needed to study in detail. In the following example, we calculated the dispersion relation of the traditional ($p = 1\,\text{mm}$, without moats) and new ($p = 3\,\text{mm}$, with moats) SIWs for understanding the difference between them. As depicted in Fig. 7, it is apparent that the SIW with moats can extend its operation bandwidth to a lower frequency; that is, the new SIW with moats has a lower cutoff frequency compared with that of the commonly used SIW with dense via-hole arrays. We may conjecture that this new SIW has a wider effective waveguide width than that of the traditional one. Regarding the attenuation constant distribution, there is no obvious difference in the attenuation constant between them.

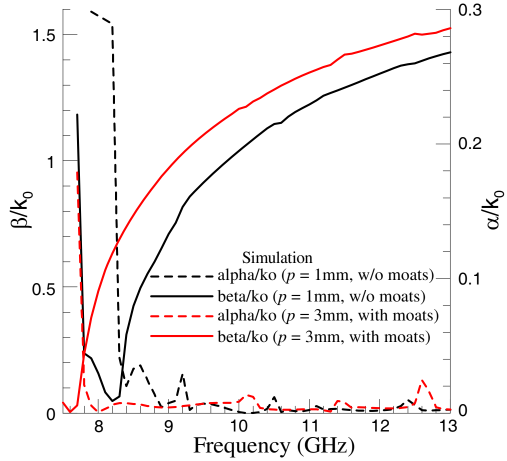

Figure 7. Calculated propagation constants, which include phase and attenuation constants, of the SIW with and without moats, respectively.

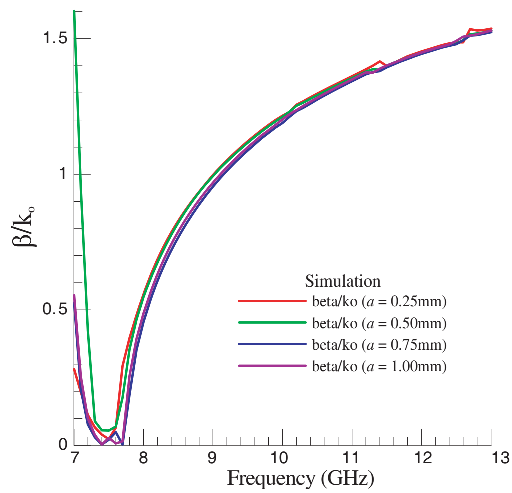

Figure 8. Calculated phase constants of the SIW with moats, where width of moat a is sweeped.

Figure 9 demonstrates variations of measured S_{21} versus frequency for various widths of moat. Here, the pitch width is 3 mm, and the other parameters are the same as those in the previous examples. From this figure, we found that the curves with moat width ranging from 0.25 mm to 1.0 mm coincide with one another. Besides, the maximum

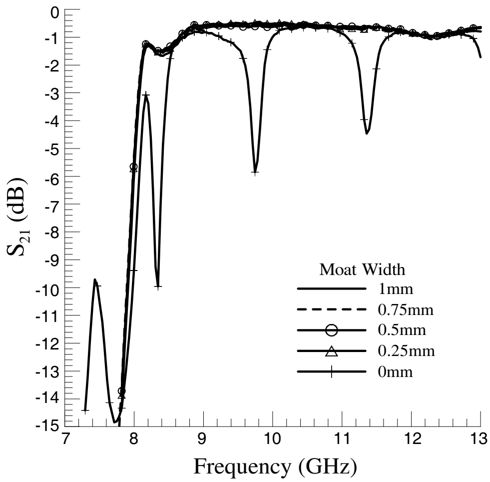

Figure 9. Measured S_{21} versus frequency for various widths of moats.

variation on the S_{21} is within 0.8 dB for all cases from 9 GHz to 13 GHz. It indicates that the effect of the moat width on the transmission characteristic is insignificant.

In addition to the previous example with 3 mm pitch, in fact, we have studied various cases with different pitches. Although not shown here, we found that the placement of moats can effectively reduce leakage loss into the parallel-plate waveguide regions. For the case with pitch width smaller or equal to 2 mm, the effect of the moat is insignificant. If the pitch is greater than 5 mm, adding moats could reduce leakage loss; however, the maximum variation on the transmission coefficient will increase. We may conjecture that the moat employed in this research is similar to a magnetic wall providing additional reflectivity in addition to that of the electric wall contributed by the via-hole array. Although the reflectivity of this magnetic wall is not as ideal as that of the perfect magnetic wall (open circuit), it indeed helps the via-hole array to stop the leakage of energy into the surrounding parallel-plate region.

4. CONCLUSION

In this paper, the new SIW equipped with moats outside the via-hole arrays were studied theoretically and experimentally. Interestingly, the placement of moats can maintain a high transmission characteristic as that of the commonly used SIW with dense via-hole arrays.

Additionally, from the dispersion relation calculation, it is interesting to find that such a new SIW with moats can lower its cutoff frequency; namely, increase its effective waveguide width. Last but not least, this scheme can further reduce electromagnetic field coupling between SIWs integrated in the same substrate.

ACKNOWLEDGMENT

This author thanks Thang Dong Hwang for his great effort in implementing substrate waveguides. The author would acknowledge National Science Council, Taiwan, Republic of China, for financial support under the contract: 95-2221-E-009-045-MY3.

REFERENCES

1. Uchimura, H., T. Takenoshita, and M. Fujii, "Development of a laminated waveguide," *IEEE Trans. Microwave Theory Technique*, Vol. 46, No. 12, 2438–2443, 1998.
2. Hirokawa, J. and M. Ando, "Single-layer feed waveguide consisting of posts for plane TEM wave excitation in parallel plates," *IEEE Transactions on Antennas and Propagation*, Vol. 46, No. 5, 625–630, 1998.
3. Deslandes, D. and K. Wu, "Integrated microstrip and rectangular waveguide in planar form," *IEEE Microwave Wireless Compon. Lett.*, Vol. 11, No. 2, 68–70, 2001.
4. Zeid, A. and H. Baudrand, "Electromagnetic scattering by metallic holes and its applications in microwave circuit design," *IEEE Trans. Microwave Theory Tech.*, Vol. 50, No. 4, 1198–1206, 2002.
5. Cassivi, Y., L. Perregrini, P. Arcioni, M. Bressan, K. Wu, and G. Conciauro, "Dispersion characteristics of substrate integrated rectangular waveguide," *IEEE Microwave Wireless Compon. Lett.*, Vol. 12, No. 9, 333–335, 2002.
6. Zhang, Y. L., W. Hong, F. Xu, K. Wu, and T. J. Cui, "Analysis of guided-wave problems in substrate integrated waveguides — Numerical simulations and experimental results," *IEEE MTT-S Int. Micro. Symp. Dig.*, Vol. 3, 2049–2052, 2003.
7. Xu, F., Y. L. Zhang, W. Hong, K. Wu, and T. J. Cui, "Finite-difference frequency-domain algorithm for modeling guided-wave properties of substrate integrated waveguide," *IEEE Transactions on Microwave Theory and Techniques*, Vol. 51, 2221–2227, 2003.

8. Xu, F. and K. Wu, "Guided-wave and leakage characteristics of substrate integrated waveguide," *IEEE Transactions on Microwave Theory and Techniques*, Vol. 53, No. 1, 66–73, 2005.
9. Wu, K., "Integration and interconnect techniques of planar and nonplanar structures for microwave and millimeter-wave circuits-current status and future trend," *Proc. Asia-Pacific Microw. Conf.*, Vol. 2, 411–416, Taiwan, R.O.C., 2001.
10. Talebi, N. and M. Shahabadi, "Application of generalized multipole Technique to the analysis of discontinuities in substrate integrated waveguides," *Progress In Electromagnetics Research*, PIER 69, 227–235, 2007.
11. Ranjkesh, N. and M. Shahabadi, "Loss mechanisms in SIW and MSIW," *Progress In Electromagnetics Research B*, Vol. 4, 299–309, 2008.
12. Sotoodeh, Z., B. Biglarbegian, F. H. Kashani, and H. Ameri, "A novel bandpass waveguide filter structure on SIW technology," *Progress In Electromagnetics Research Letters*, Vol. 2, 141–148, 2008.
13. Wang, R., L. S. Wu, and X. L. Zhou, "Compact folded substrate integratedwaveguide cavities and bandpass filter," *Progress In Electromagnetics Research*, PIER 84, 135–147, 2008.
14. Ismail, A., M. S. Razalli, M. A. Mahdi, R. S. A. R. Abdullah, N. K. Noordin, and M. F. A. Rasid, "X-band trisection substrate-integrated waveguide quasi-elliptic filter," *Progress In Electromagnetics Research*, PIER 85, 133–145, 2008.
15. Zhang, X. C., Z. Y. Yu, and J. Xu, "Novel band-pass substrate integrated waveguide (SIW) filter based on complementary split ring resonators (CSRRs)," *Progress In Electromagnetics Research*, PIER 72, 39–46, 2007.
16. Zhong, C. L., J. Xu, Z. Y. Yu, M. Y. Wang, and J. H. Li, "Half mode substrate integrated waveguide broadband bandpass filter," *Progress In Electromagnetics Research Letters*, Vol. 4, 131–138, 2008.
17. Han S. H., X. L. Wang, Y. Fan, Z. Q. Yang, and Z. N. He, "The generalized chebyshev substrate integrated waveguide diplexer," *Progress In Electromagnetics Research*, PIER 73, 29–38, 2007.
18. Lin, S., S. Yang, and A. E. Fathy, "Development of a novel UWB vivaldi antenna array using SIW technology," *Progress In Electromagnetics Research*, PIER 90, 369–384, 2009.